ACS Sustainable Chemistry & Engineering

Research Article

Cite This: ACS Sustainable Chem. Eng. 2019, 7, 1769−1777

pubs.acs.org/journal/ascecg

Synergistic Aqueous Biphasic Systems: A New Paradigm for the "One-Pot" Hydrometallurgical Recovery of Critical Metals

Nicolas Schaeffer,[†,§] Matthieu Gras,[‡,§] Helena Passos,[†] Vijetha Mogilireddy,[‡] Carlos M. N Mendonça,[†] Eduarda Pereira,[†] Eric Chainet,[‡] Isabelle Billard,[‡] João A.P. Coutinho,*[,†] and Nicolas Papaiconomou*[,‡]

[†]CICECO, Aveiro Institute of Materials, Department of Chemistry, University of Aveiro, 3810-193 Aveiro, Portugal

[‡]LEPMI, Universite Grenoble-Alpes, 1130 Rue de la Piscine, F-38000 Grenoble, France

Supporting Information

ABSTRACT: An acidic aqueous biphasic system (AcABS), in which the inorganic salt component of a traditional aqueous biphasic system (ABS) is replaced by the inorganic acid inherently present in typical hydrometallurgical leachate solution, is shown to selectively separate cobalt from nickel, a separation relevant to the recycling of nickel metal hydride (NiMH) batteries. To overcome the limitation of electrodeposition in the presence of high acid concentration, a mixed ABS−AcABS approach is developed in which HCl is partially substituted by addition of a predictable amount of NaCl. This synergistic ABS−AcABS retains the metal extraction efficiency of AcABS while diminishing the acid concentration required to induce phase separation as well as its distribution to the ionic-liquid-rich phase. Selective deposition of cobalt in the presence of coextracted manganese impurities was achieved in AcABS, ABS, and ABS−AcABSs. The morphology and composition of the obtained deposits as well as the Faradaic efficiency of the process can be altered by varying the NaCl to HCl ratio and water content, resulting in highly tailored cobalt deposits. These results highlight the potential of AcABS-derived systems as a new extraction−separation platform for the integrated hydrometallurgical treatment of critical metals, from leaching to electrodeposition.

KEYWORDS: *Acidic aqueous biphasic systems, Critical metals, Ionic liquids, Waste electrical and electronic equipment, Electrodeposition*

INTRODUCTION

The extraction, separation, and purification of critical metals from complex matrices such as minerals or electronic wastes are technologically challenging, often requiring a series of demanding processing steps. A traditional flowsheet for the hydrometallurgical treatment of metal feedstocks follows a series of concentration (leaching), purification (solvent extraction), and refining (electrodeposition or precipitation) stages.[1−5] Process intensification, i.e., the ability to conduct multiple hydrometallurgical operations within a single processing unit, is of great interest industrially as this can reduce the economic and environmental impact associated with metal consumption. In this context, a sustainable, effective, and affordable metal extraction process is an issue of critical importance. To alleviate metal criticality and reduce the environmental impact of mining operations, the development of a simple, robust, and flexible platform is of particular relevance for the recycling of metals from secondary "ores".

We recently proposed a "one-pot" solution for the simultaneous leaching and selective extraction of various critical metals using an ionic-liquid-based acidic aqueous biphasic system (AcABS).[6] Ionic liquids (ILs) are salts composed of asymmetric ions with disperse charge that are liquid at room temperature.[7] In the newly reported AcABS composed of the IL tributyltetradecyl phosphonium chloride ($[P_{44414}]Cl$), the very acid present in the leaching solution was used to salt-out the IL. This is markedly different from conventional aqueous biphasic systems (ABSs), such as the previously reported $[P_{44414}]Cl$−NaCl-based ABS for metal extraction,[8] in which the molar entropy of hydration of an inorganic salt dictates the formation of a reversible biphasic system composed of a salt-rich phase and organic-rich phase.[9] Performing the extraction in aqueous media reduces the overall environmental impact associated with IL application as (i) lower quantities are required compared to solvent extraction, (ii) hydrophilic ILs are less toxic and more biodegradable than their hydrophobic counterparts, and (iii) mass transfer

Received: November 6, 2018
Revised: December 10, 2018
Published: December 11, 2018

DOI: 10.1021/acssuschemeng.8b05754
ACS Sustainable Chem. Eng. 2019, 7, 1769−1777

properties are significantly improved due to the lower solution viscosity, resulting in faster extraction kinetics.[10−14]

In this work, the scope AcABS processes is extended to investigate the extraction and separation of Co(II), a critical metal,[15] from Ni(II) and Mn(II)—a separation relevant to the recycling of nickel metal hydride and lithium-ion batteries.[16] To this end, a mixed ABS−AcABS approach is proposed in which the HCl content required to induce phase separation in AcABS is predictably substituted by small amounts of NaCl, further accentuating the versatility of the proposed approach. Synergistic ABS−AcABSs retain the advantages of AcABS while diminishing the acid concentration required to induce phase separation as well as its distribution to the IL-rich phase. This enables the use of more environmentally friendly operating conditions and facilitates the subsequent metal deposition from the IL-rich phase. Selective deposition of Co(II) is optimized as a function of various parameters including water content, HCl concentration, and NaCl concentration. The ability to directly deposit metals from the IL-rich phase opens the possibility for a fully integrated approach to the leaching, separation, and deposition of critical metals from complex sources.

METHODOLOGY

Materials and Instrumentation. A detailed description of the compounds used as well as the instrumentation employed is provided in the Methodology section of the Supporting Information. The chemicals were used as received without further purification.

Determination of Mixed ABS−AcABSs for Metal Extraction. It is important to emphasize that three different separation systems are employed in this work: two ternary systems composed of $[P_{44414}]Cl-HCl-H_2O$ (AcABS) and $[P_{44414}]Cl-NaCl-H_2O$ (ABS), respectively, and a quaternary system $[P_{44414}]Cl-HCl-NaCl-H_2O$ referred to as ABS−AcABS. The phase diagrams for the quaternary system ABS−AcABS containing a fixed NaCl concentration (1, 2, and 4 wt %) were determined through the cloud point titration method in a temperature-controlled cell at 298 K under agitation and atmospheric pressure. The concentration of NaCl was identical (1, 2, and 4 wt %) in all solutions used to keep its concentration constant throughout the cloud point titration procedure. The quaternary system compositions were determined by the weight quantification of all components added within an uncertainty of $\pm 10^{-3}$ g. The detailed experimental procedure adopted is described in a previous work.[17] The extraction and separation of Co(II) from Ni(II) and Mn(II) in different ABS−AcABS mixtures of total mass 5 g containing 30 wt % $[P_{44414}]Cl$ were studied as a function of the HCl to NaCl ratio. A mixed metal ion solution containing 0.1 mol L^{-1} $CoCl_2{\cdot}6H_2O$, 0.1 mol L^{-1} $NiCl_2{\cdot}6H_2O$, and 0.1 mol L^{-1} $MnCl_2{\cdot}4H_2O$ was used for all experiments. Solutions were mechanically agitated for 5 min at 298 K until the complete dissolution of the IL. The resulting mixture was left to phase separate for 60 min in a thermostatic bath at 298 K. The volume of each phase of the ABS−AcABS was measured, and aliquots of the upper and lower phases were collected for metal concentration analysis by inductively coupled plasma optical emission spectroscopy (ICP-OES) after appropriate dilution. The chloride, acid, and water content of the IL-rich phase (top phase) was also determined after separation of the phases. The extraction efficiency (%EE) was calculated as follows:[6]

$$\%EE = \frac{\frac{[M]_0 V_{initial}}{V_{low}} - [M]_{low}}{[M]_0} \times 100 \quad (1)$$

where $[M]_0$ is the initial metal concentration of the metal in solution before extraction (i.e., before addition of the IL). $V_{initial}$ is the volume in mL of the mixture before extraction while V_{low} is the volume, expressed in mL, of the lower phase after extraction. $[M]_{low}$ is the concentration of the metal ion in the lower phase after extraction.

Electrodeposition of Co(II) from ABS−AcABS. Electrochemical investigations including chronoamperometry and cyclic voltammetry (CV) were carried out using a Metrohm Autolab potentiostat controlled with GPES software. A three-electrode system was used consisting of a glassy carbon (GC) working electrode (3 mm diameter), an iridium counter electrode, and a silver chloride (Ag/AgCl) reference electrode. The working electrode was polished with diamond paste, rinsed, and dried prior to all measurements. All cyclic voltammograms of single 0.1 mol L^{-1} Co(II) aqueous solutions were obtained at 298 K and at a scanning rate of 0.01 V s^{-1} with varying $[P_{44414}]Cl$ (from 0 to 20 wt %) and HCl concentrations (0−8 mol L^{-1}).

Chronometric deposition experiments were performed in the following three systems: ABS, AcABS, and ABS−AcABS (with and without the addition of water). Compositions of all systems are presented in Table S1 in the SI. After extraction from a single metal solution containing 0.1 mol L^{-1} of $CoCl_2{\cdot}6H_2O$ or a mixed solution of 0.1 mol L^{-1} of $CoCl_2{\cdot}6H_2O$, $NiCl_2{\cdot}6H_2O$, and $MnCl_2{\cdot}4H_2O$, the IL-rich phase was isolated from the aqueous one. CV experiments were carried out under agitation in the potential range from −2.50 to 2.00 V versus Ag/AgCl at a scan rate of 0.01 V s^{-1}. Electrodeposition of metals was undertaken by chronoamperometry agitation at a fixed potential of −2.00 V versus Ag/AgCl during 1 h. The three systems, namely, AcABS, ABS, and ABS−AcABS, depicted in Table S1 were studied. A fourth system was considered to investigate the impact of the water content on the deposition. After separation and isolation of the phases from the system ABS−AcABS, the IL-rich phase was diluted in a minimum of water (0.2 g of water per gram of isolated IL-rich phase) until the solution color transitioned from deep blue to light red. This well-known color change is due to the transition of blue chloride complexes ($CoCl_4^{2-}$ or $CoCl_3^{2-}$) to the formation of a red cobalt hexahydrate complex, $Co^{2+}(H_2O)_6$.[18] This system is referred to as "ABS−AcABS-diluted" in this work.

Obtained deposits were analyzed by SEM−energy dispersive spectroscopy (SEM−EDS) for single metal extractions. Metallic deposits obtained after selective deposition of cobalt in multi-elemental solutions were analyzed through X-ray diffraction (XRD). In the latter case, the metal was fully leached in 5 mL of 4 mol L^{-1} nitric acid (HNO_3) to investigate (i) the purity of the metal and (ii) the Faradaic efficiency of the electrodeposition (E_F). The Faradaic yield corresponds to the ratio between the experimental and theoretical conversion of Co(II) to Co(0) during electrodeposition. E_F was calculated according to the following equation:

$$E_F = \frac{C_{Co} \times V_{HNO_3}}{\frac{\int_0^t I(t)\,dt}{nF}} \times 100 \quad (2)$$

where C_{Co} represents the concentration of cobalt in mol L^{-1} in the aqueous phase containing nitric acid, used to leach the deposits. V_{HNO_3} is the volume of the nitric acid solution in L. I (A) represents the current produced during chronoamperometry measurements for a given time t in seconds. F and n stand for the Faraday constant and the number of moles of electrons exchanged during the reduction, respectively.

RESULTS AND DISCUSSION

Development of Mixed ABS−AcABSs for Metal Extraction. The innovation of AcABS lies in its ability to extract metals directly from leachates just by adding a carefully selected IL. However, optimal extraction and separation of Co(II) in the $[P_{44414}]Cl-HCl-H_2O$ AcABS were shown to occur for highly concentrated solutions of HCl above 8 mol L^{-1} or ∼25 wt %, considerably more concentrated than most common leaching solutions (cf. Figure S1 of the SI). A full description Co(II), Ni(II), and Mn(II) extraction in AcABS is provided in the "Metal Extraction in the $[P_{44414}]Cl-HCl-H_2O$ AcABS" section in the SI. This includes the effect of HCl

DOI: 10.1021/acssuschemeng.8b05754
ACS Sustainable Chem. Eng. 2019, 7, 1769−1777

concentration in AcABS on the partition of $[H_3O]^+$, Cl^-, and H_2O to the IL-rich phase (Table S2, SI); the IL-rich phase viscosity before and after metal extraction (Figure S2, SI); and the influence of Co(II) feed concentration on the extraction efficiency and system properties of AcABS (Figures S3 and S4, SI).

However, the addition of extra HCl to leachates to induce AcABS formation and the efficient extraction of Co(II) is not realistic from an industrial perspective because of (i) the corrosivity of HCl and (ii) the increased cost of solution neutralization after extraction. Furthermore, even small HCl concentrations can inhibit the subsequent electrodeposition of Co(II) due to the narrowing of the electrochemical window caused by the reduction of $[H_3O]^+$ (cf. Figure S5 in the SI). $[P_{44414}]Cl$ was shown to form ABS with a wide range of chloride salts.[19] As such, we propose a mixed ABS–AcABS using mixtures of HCl/NaCl capable of efficiently separating Co(II) from Ni(II) and Mn(II) from any chloride-containing aqueous solution, even at low HCl concentrations. It is important to stress that some degree of solution acidity is required to leach metals and to prevent metal hydrolysis common at the high pH of typical ABS.

The binodal curves for $[P_{44414}]Cl–HCl–H_2O$ systems containing 1, 2, and 4 wt % NaCl at T = 298 K are presented in Figure 1A. As expected from the lower cloud point of the

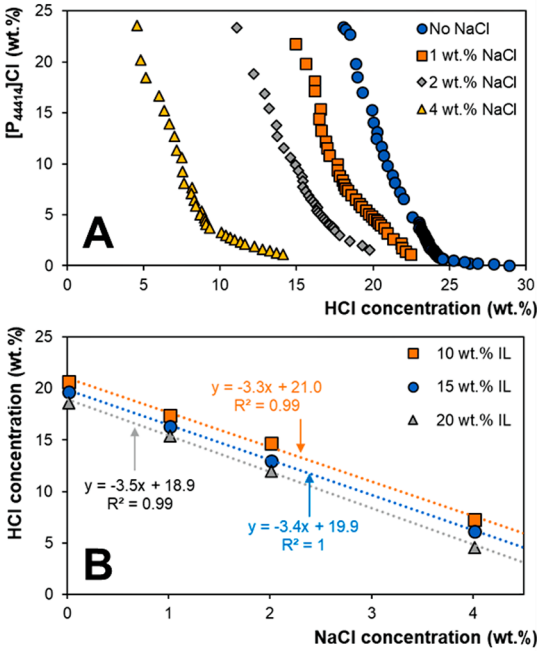

Figure 1. (A) Effect of NaCl concentration on the binodal curve of the $[P_{44414}]Cl–HCl–H_2O$ system at 298 K (binodal data is provided in Table S3 in the SI). (B) Reduction in the HCl concentration required to induce phase separation at a fixed NaCl concentration for 10, 15, and 20 wt % $[P_{44414}]Cl$.

$[P_{44414}]Cl–NaCl–H_2O$ system compared to that of HCl,[19] the addition of a small concentration of NaCl results in a large decrease in the corresponding HCl concentration required to induce phase separation. For 15 wt % $[P_{44414}]Cl$, approximately 21 wt % HCl is required compared to 6.5 wt % HCl for a mixed ABS–AcABS containing 4 wt % NaCl. An additional benefit of the presented ABS–AcABS is the predictable shift in the binodal position with increasing NaCl concentration as shown in Figure 1B. For $[P_{44414}]Cl$ concentrations above 5 wt %, the binodals in Figure 1A are roughly parallel. This allows the following simplification to be made: the addition of 1 wt % NaCl decreases the HCl requirement by approximately 3.4 wt %. The proposed linear correlation is only valid for ABS–AcABS containing up to of 4 wt % NaCl. Addition of NaCl above 4 wt % does not provide the same relative HCl decrease as below this salt concentration (Figure S6 in the SI). This appears as the limit for the synergistic effect of NaCl with HCl in ABS–AcABS.

The partition of Co(II), Ni(II), and Mn(II) from a multielement solution containing 0.1 mol L^{-1} of each respective metal ion was attempted for eight ABS–AcABSs at different HCl:NaCl ratios (T = 298 K). The system compositions are given in Table S4 of the SI, and their respective metal extraction efficiency and the concentration of Cl^-, $[H_3O]^+$, and H_2O in the IL-rich phase after extraction and phase separation are presented in Figures 2 and 3 and Table

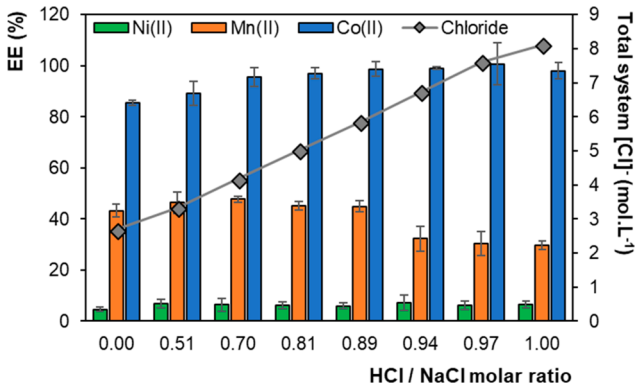

Figure 2. Co(II), Mn(II), and Ni(II) extraction efficiencies in ABS–AcABS with varying NaCl to HCl concentrations at 298 K. System compositions are provided in Table S4 of the SI.

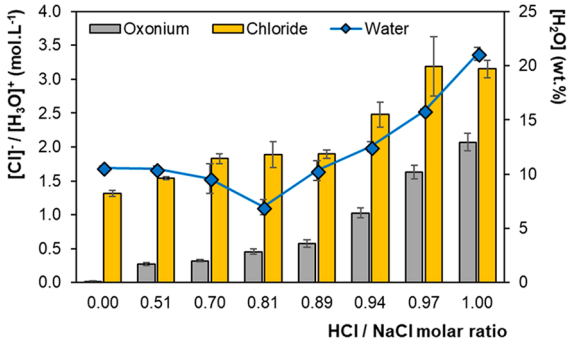

Figure 3. Concentration of acid ($[H_3O]^+$), chloride anion, and water in the $[P_{44414}]Cl$-rich phase after metal extraction in ABS–AcABS with varying NaCl to HCl concentrations at 298 K. System compositions, including the partition behavior of the acid and water to the IL-rich phase, are provided in Table S4 of the SI.

S4. The concentration of the $[P_{44414}]^+$ cation in the aqueous phase was found to be below the detection limit for all tested systems and is not included. The results in Figure 2 show that, for all systems, there is little variation in the extraction efficiency of the studied metal ions as one moves from ABS to AcABS despite the large variation in the total chloride concentration. Co(II) was extracted to the IL-rich phase while Ni(II) remained in the aqueous phase, and Mn(II)

DOI: 10.1021/acssuschemeng.8b05754
ACS Sustainable Chem. Eng. 2019, 7, 1769–1777

partitioned between the two, with a slight increase in Mn(II) extraction at higher NaCl concentrations. These results are in accordance with previously reported Co(II) and Ni(II) extraction from $[P_{44414}]Cl–NaCl–H_2O$ ABS and $[P_{44414}]Cl–HCl–H_2O$ AcABS[6,8] as well as those using hydrophobic phosphonium-based ILs in traditional liquid–liquid extraction.[13,14,16,20]

ILs incorporating quaternary phosphonium cations are known to extract anionic metal complexes such as those formed by Co(II), Cu(II), Fe(III), Pd(II), or Pt(IV) at high halide concentrations through the formation of a hydrophobic pair between the anionic metal complex and the cation of the IL.[6,8,13,14,20,21] Ni(II) exhibits a limited coordination with chloride anions, highlighted by the low complexation constant of $NiCl^+$ ($k_1^{Ni^{2+}} = 0.07$).[18] The inability of Ni(II) to form anionic chloro-complexes in water results in low extraction yields due to its inability to form an ion pair with the IL cation. The intermediate complexation constant of Mn(II) with Cl^- ($k_1^{Mn^{2+}} = 0.33$) compared to Ni(II) and Co(II) ($k_1^{Co^{2+}} = 0.40$)[18] is reflected in its extraction efficiency (Figure 2). The speciation of Co(II) is highly dependent on the ratio of Co(II) concentration to chloride concentration in solution; the anionic species $CoCl_3^-$ and $CoCl_4^{2-}$ can be found at high HCl concentrations.[18] This transition from $Co(H_2O)_6^{2+}$ found in aqueous solutions to negatively charged Co(II) complexes can be visually observed as the solution changes color from pinkish red to deep blue, the same as the color of the IL-rich phase after extraction. A previous study on the extraction of Co(II) using $[P_{44414}]Cl$ confirmed that Co(II) is predominantly extracted as the $CoCl_4^{2-}$ species within the IL phase.[6,8] The speciation of Co(II) is highly relevant for its subsequent electrodeposition from IL solutions and will be addressed further on.[22]

On a molar basis, significantly less Cl^- is required to induce ABS phase separation and Co(II) extraction when NaCl is employed compared to HCl. NaCl was shown to be a more efficient salting-out agent than HCl for the liquid–liquid demixing of $[P_{44414}]Cl$-based ABS.[19] Extraction of Co(II) is close to quantitative for a HCl:NaCl ratio of 0.7 or greater. It is postulated that, in such systems, the Cl^- provides the necessary chloride to form anionic chloro-cobalt complexes while the greater salting-out effect of Na^+ compared to that of $[H_3O]^+$ promotes the transition of the less hydrophilic $CoCl_3^-$ and $CoCl_4^{2-}$ species to the IL-rich phase. This supports the claim that a mixed ABS–AcABS for metal extraction combines the advantages and flexibility of AcABS with those of ABS with no loss in metal extraction efficiency.

The partition behavior of the acid and water to the IL-rich phase in mixed ABS–AcABS presents an interesting behavior based on the ratio of HCl to NaCl as shown in Figure 3. The water content of the IL-rich phase is low for all the studied systems, decreasing down to a minimum of 7 wt % H_2O for an ABS–AcABS composition of 30 wt % $[P_{44414}]Cl$, 10.8 wt % HCl, and 4.0 wt % NaCl. The water content increases as NaCl is substituted by HCl from 10.6 wt % in ABS and reaching 21.1 wt % for the pure AcABS in line with the greater salting-out potential of NaCl compared to HCl.[19] Furthermore, the acid concentration in the IL-rich phase does not significantly increase while NaCl is the primary driver (HCl:NaCl molar ratio <0.89) for the phase separation of ABS–AcABS. From the presented results, two conclusions can be inferred of great relevance for the subsequent electrodeposition of Co(II) from a $[P_{44414}]Cl$-rich phase. First, a mixed ABS–AcABS can be predictably tuned with little appreciable variation in metal extraction compared to simple ABS or AcABSs. Second, a compromise is required in the HCl to NaCl ratio of ABS–AcABS. Higher NaCl concentrations reduce the acid and chloride migration to the IL-rich phase at the expense of a lower water content compared to simple AcABS. The high viscosity of loaded $[P_{44414}]Cl$ solutions can reduce the diffusion of Co(II) as well as cause losses during manipulation. However, minimizing the acid concentration will facilitate the deposition of Co(II) from $[P_{44414}]Cl$ solutions. An additional consideration is that the water content, and therefore the viscosity, of the loaded $[P_{44414}]Cl$-rich phase once isolated, can be controlled by dilution with water.

Electrochemical Behavior of Co(II) in ABS–AcABSs. Upon demonstration of the separation of Co(II) from Ni(II) and Mn(II) in AcABS and ABS–AcABS as well as the partitioning of the system components relevant to the subsequent deposition of Co(II), the electrochemical behavior of the studied system is now investigated. The influence of the hydrophilic $[P_{44414}]Cl$ in aqueous solutions on the reduction potential of Co(II) is presented in Figure 4. The presence of the IL in aqueous solution lowers the kinetics of water to hydrogen reduction (cf. Figure 4A), in line with the wide

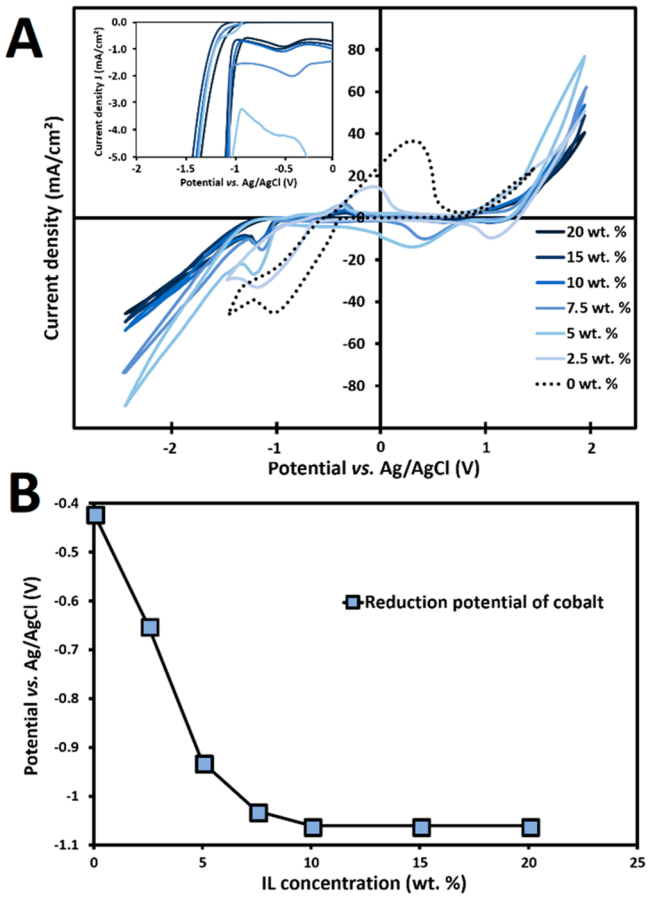

Figure 4. (A) CV experiments at a 0.01 V s^{-1} scan rate of various solutions containing 0.1 mol L^{-1} of Co(II) and concentration of $[P_{44414}]Cl$ ranging between 0 (black dotted line) and 20 (light to dark blue colors) wt %. (B) Evolution of the inset peak corresponding to the reduction of Co(II) to Co(0) as a function of the concentration of $[P_{44414}]Cl$.

DOI: 10.1021/acssuschemeng.8b05754
ACS Sustainable Chem. Eng. 2019, 7, 1769–1777

electrochemical window of phosphonium-based ILs.[23,24] Co(II) is known to reduce to metallic cobalt at a potential of −0.28 V versus NHE, that is, −0.50 V versus Ag/AgCl.[25] In accordance with the literature, the CV of an aqueous 0.1 mol L^{-1} Co(II) solution (Figure 4A, dashed line) presents an inset reducing peak at −0.42 V and a minimum at −1.0 V versus Ag/AgCl. A large oxidation peak is also observed from 0.42 to 0.59 V versus Ag/AgCl, confirming that cobalt can be oxidized reversibly. The addition of increasing amounts of $[P_{44414}]Cl$ from 0 to 10 wt % IL results in a decrease in the cathodic peak potential for cobalt (E^{red}_{Co}) from −0.42 to −1.06 V versus Ag/AgCl. When the concentration of IL exceeds 10 wt %, the reduction peak potential remains constant (cf. Figure 4B). This shift in the reduction peak is a strong indication of a change in the complexation of Co(II) in the presence of the chloride anions from the IL. The anionic cobalt complexes $CoCl_3^-$ and $CoCl_4^{2-}$ are the predominant complexes reported in chloride-based ILs.[13,14,22,26] Furthermore, while the $CoCl_3^-$ was shown to be electrochemically active in ILs, the complex $CoCl_4^{2-}$ was not.[22] This suggests that a high chloride concentration is inhibiting the deposition of Co(0). This is in accordance with the Nernst law, which states that changes in the speciation have an influence on the standard reduction potential of metallic species.

However, complexation of chlorides is insufficient to explain the magnitude of the shift in the reduction potential. The electrochemical kinetic behavior of nickel electrodeposition was previously studied in acidic aqueous phases and led to the intermediate formation of Ni(OH) adsorbed species.[27−29] Similarly, cobalt is assumed to present the following reduction mechanism in water:

$$Co^{2+} + e^- + OH^- \leftrightarrow Co(OH)_{ads} \quad (3)$$

$$Co(OH)_{ads} + e^- \leftrightarrow Co + OH^- \quad (4)$$

Elevated concentrations of ILs could inhibit the formation of the intermediate complex cobalt(I) hydroxide adsorbed species and therefore reduce the kinetic of reduction of Co(II).

The intensity of all reduction peaks decreases with the increasing IL concentration because of the higher viscosity and therefore lower kinetics of the IL-concentrated systems compared to the pure water system. Finally, an unveiled trend can be observed for mixtures containing 5 wt % $[P_{44414}]Cl$ or more with the emergence of a small reduction peak close to −0.5 V versus Ag/AgCl (Figure 5A, inset). This is attributed to the reduction of Co(II) to Co(I). ILs provide a better environment for the stabilization of intermediate metal oxidation states compared to water. For example, the presence of water was shown to significantly affect the voltammetric behavior of Co(II) in the ethylammonium nitrate IL and the oxidation of Co(II) to Co(III).[30]

CV analysis at a scan rate of 0.01 V s^{-1} and 298 K on a GC working electrode was carried out in the four systems AcABS, ABS, and ABS−AcABS (both undiluted and diluted) after extraction from 0.1 mol L^{-1} Co(II) solutions. The solution compositions of the studied systems are listed in Table S1. The CV scans are presented in Figure 5. Electrodeposition of Co(II) was performed during 1 h on a GC electrode under agitation. The electrodes were qualitatively and semiquantitatively analyzed via SEM-SE and SEM-ESD, respectively. The morphology and composition of the obtained deposits are presented in Figure 6 and Table 1, respectively.

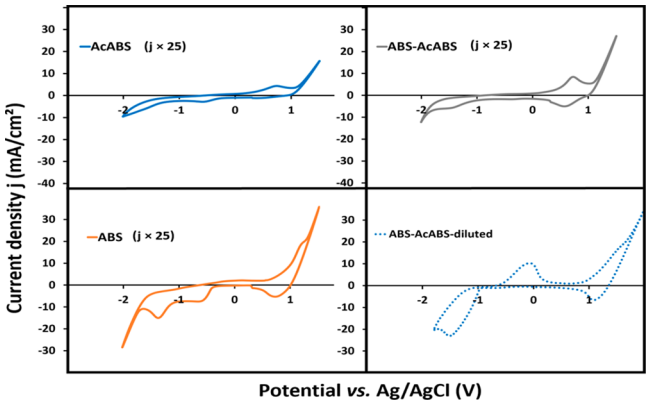

Figure 5. CV of various systems after extraction of cobalt in an aqueous solution containing 0.1 mol L^{-1} Co(II). Scanning rate: 0.01 V s^{-1}. Current densities (J) are multiplied by 25 for the ABS, AcABS, and ABS−AcABSs.

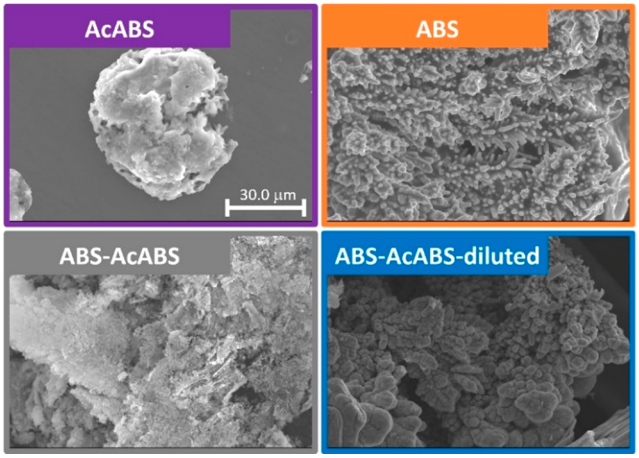

Figure 6. SEM-SE images (magnification ×1000) of working electrodes after 1 h of electrodeposition at −2.00 V vs Ag/AgCl.

Table 1. Elemental Analysis of the Electrodeposited Deposits Obtained in ABS, AcABS, and ABS−AcABSs (Undiluted and Diluted) after Extraction from Solutions Containing 0.1 mol L^{-1} Co(II)

system	elemental analysis (mol %)		
	Co	Cl	P
ABS	98.9 ± 12.3	1.1 ± 0.5	
AcABS	52.7 ± 23.3	44.7 ± 18.3	2.6 ± 1.6
ABS−AcABS	92.6 ± 12.5	6.9 ± 6.3	0.5 ± 0.1
ABS−AcABS-diluted	95.6 ± 16.3	3.3 ± 2	1.1 ± 0.6

Starting with the ABS, first reported by Onghena et al.[8] composed of $[P_{44414}]Cl−NaCl−H_2O$, a reduction peak (Co(II) to Co(0)) with an onset point at −1.07 V versus Ag/AgCl can be observed (Figure 5, orange line). This is in full agreement with our previous result showing that E^{red}_{Co} = −1.06 V versus Ag/AgCl for systems containing 10 wt % or more $[P_{44414}]Cl$. After inducing a potential of −2.00 V versus Ag/AgCl to the solution, EDS analysis of the obtained deposit on the GC electrode surface indicates a high-purity cobalt deposit of 98.9 mol % (Table 1). No significant quantities of chloride or phosphonium are recorded. The morphology of the obtained deposit is that of micrometer-scale dendrites, characteristic of metallic cobalt in aqueous solutions.[31] Despite

DOI: 10.1021/acssuschemeng.8b05754
ACS Sustainable Chem. Eng. 2019, 7, 1769−1777

the lack of a visible Co(0) reduction peak in the $[P_{44414}]Cl-HCl-H_2O$ AcABS (Figure 5, purple line), small particles were identified on the GC electrode after electrodeposition. This is a direct consequence of the large concentration of acid after extraction in the top phase ($[H_3O]^+ = 3.0 \pm 0.26$ mol L^{-1}). In such an acidic environment, Co(0) particles can be leached back in the aqueous solution after deposition. Two concomitant but opposing phenomena emerge: (i) the reduction of Co(II) at the negative overpotential and (ii) the oxidation of Co(0) due to the HCl concentration. As a result, the particle seen in Figure 6 is composed of only 52.7 mol % cobalt and 44.7 mol % chloride, characteristic of an ongoing leaching phenomenon.

To avoid leaching just after the electrodeposition step, a mixed ABS−AcABS containing $[P_{44414}]Cl-NaCl-HCl-H_2O$ is evaluated (composition provided in Table S1). As shown in Figure 3, the partial substitution of HCl by NaCl reduces the $[H_3O]^+$ concentration of the IL-rich phase while maintaining the required solution acidity to perform the leaching of metals. This system was studied both in its undiluted and diluted form to establish the impact of water, and therefore Co(II) complexation, on the quality of the Co(0) deposits. In the CV of undiluted ABS−AcABS, E_{Co}^{red} appears at −1.12 V versus Ag/AgCl (Figure 5, gray line), similar to that obtained in the ABS. The composition of the obtained deposit is 92 mol % cobalt and only 7 mol % chloride. This represents a significant increase in the deposit purity compared to that obtained in AcABS. The presence of Cl^- is assigned to (i) the presence of residual $[P_{44414}]Cl$ in the final deposit and to (ii) the small leaching effect from the persistent presence of HCl ($[H_3O]^+ = 0.35 \pm 0.04$ mol L^{-1}). SEM-SE analysis of the working electrode surface after deposition reveals its complete coverage by a large layer of deposit (cf. Figure 6). The deposit presents a sheetlike structure with no observable dendrites. This is probably due to the etching of the deposit surface by the remaining HCl after oxidation of Co(0) present in the dendritic structures of high surface area.

For a better understanding on the role of water in the studied system, the IL-rich phase (top phase) of the mixed system ABS−AcABS was isolated after extraction and diluted (0.2 g of water per gram of isolated IL-rich phase). The system was diluted through dropwise addition of water until a shift in the solution color from blue to light red was observed. Upon varying of the water content of the IL-rich phase after AcABS extraction, essentially transitioning from a water in IL environment to IL as electrolytes in aqueous solutions, the mass transport and interfacial structure at the electrode can be altered resulting in potentially different deposit properties.[32,33] An additional positive effect of dilution on the Faradaic efficiency is the change in Co(II) coordination from chloro-cobalt complexes to Co(II) hexahydrate. Dilution of the system results in a positive shift in the onset of the reduction peak from −1.12 V versus Ag/AgCl for ABS−AcABS to −0.90 V versus Ag/AgCl for ABS−AcABS-diluted. The dilution influences the complexation of cobalt-chloride complexes, thereby increasing the reduction potential in accordance with Nernst's law. A deposit composed of large dendrites was visually observed, further confirmed by SEM-SE (cf. Figure 6). Elemental analysis of the deposit highlights a quasipure material composed of 95.5 mol % cobalt. In light of these results, the $[P_{44414}]Cl-NaCl-HCl-H_2O$ mixture stands out as a promising medium for the recovery of metallic cobalt. The morphology and composition of the obtained deposits can be altered by varying the NaCl to HCl ratio and water content, resulting in highly tailored cobalt deposits. However, extraction results displayed in Figure 2 indicate that up to 40 wt % Mn(II) can be coextracted with Co(II). The question of the selectivity of such a process, starting from an aqueous solution containing a mixture of Co(II), Mn(II), and Ni(II), thus arises.

Selective Electrodeposition of Co(II) from Ni(II) and Mn(II). After extraction of a mixture of 0.1 mol L^{-1} Co(II), Ni(II), and Mn(II) from ABS and ABS−AcABSs (Table S1 of the SI), chronoamperometry experiments at −2 V versus Ag/AgCl were carried out to selectively reduce cobalt to its metallic state. Results are given in Figure 7. Current densities

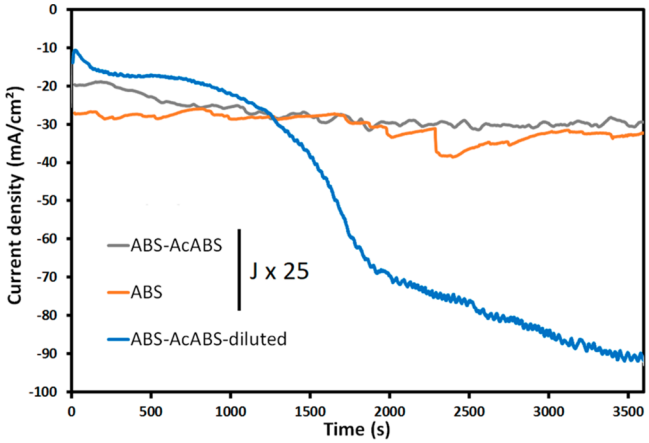

Figure 7. Chronoamperometry experiments using a potential of −2.00 V vs Ag/AgCl for 1 h. Current densities (J) are multiplied by 25 for the ABS and ABS−AcABSs.

for all experiments suffer from some oscillations as a result of hydrogen evolution from the reduction of water and/or of $[H_3O]^+$. The current density slowly decreases with time during deposition in all systems, characteristic of metallic deposition. The reduction of a conductive material such as cobalt can increase the surface area of the electrode and thus the current density in absolute value. This phenomenon is particularly pronounced in the ABS−AcABS-diluted system where the current density is multiplied by a factor of 8 in 1 h. The lower viscosity and chloride complexation of this system are beneficial for an efficient deposition of metals. Quantitative compositional analysis of the deposits for the systems is presented in Figure 7, and their respective Faradaic efficiencies are displayed in Table 2.

For all studied systems, no traces of Mn(II) and Ni(II) were recorded, confirming that solely Co(II) is reduced as a metallic species. This is to be expected as Ni(II) is not extracted to the IL-rich phase (cf. Figure 1), and Mn(II) presents a reduction potential of −1.41 V versus Ag/AgCl, lower than that of Co(II) (−0.5 V versus Ag/AgCl).[25] The efficiency of Co(II) reduction is low in the undiluted ABS and ABS−AcABSs with a final deposit mass of 0.30 and 0.29 mg, respectively. Faradaic efficiencies indicate that around 30% of the electrons generated by the potentiostat are devoted to the reduction of Co(II) to metallic Co(0) in these systems. Inducing a potential of −2.00 V versus Ag/AgCl results in an important reduction of water and/or proton to hydrogen. The low energetic yields hinder the industrial application for such processes.

Deposition yields are significantly improved after dilution, with close to a 24-fold increase in the deposit mass to 7.2 mg

DOI: 10.1021/acssuschemeng.8b05754
ACS Sustainable Chem. Eng. 2019, 7, 1769−1777

Table 2. ICP Analysis Performed for ABS, ABS−AcABS, and ABS−AcABS-diluted Systems[a]

deposit composition	extraction systems		
	ABS−AcABS	ABS	ABS−AcABS-diluted
Co (mg)	$0.30 \pm 5 \times 10^{-3}$	$0.29 \pm 5 \times 10^{-3}$	7.2 ± 0.1
Mn (mg)	$<5 \times 10^{-3}$	$<5 \times 10^{-3}$	$<5 \times 10^{-3}$
Ni (mg)	$<5 \times 10^{-3}$	$<5 \times 10^{-3}$	$<5 \times 10^{-3}$
E_F (%)	28.9	31.6	59.7
Co electroplated (mol %)	0.91	0.82	2.51

[a]The composition of the deposits and Faraday efficiencies (E_F) are given for all systems.

in the system ABS−AcABS-diluted. This results in a 2-fold increase in the Faradaic efficiency to a value of 59.7%. The Faradaic yields reported here are reasonably satisfying and were obtained without any optimization of the electrochemical process. At −2 V versus Ag/AgCl, water or $[H_3O]^+$ present in the medium is expected to be reduced significantly. Carrying out the experiments at a more positive potential would most probably lead to better yields due to a less pronounced reduction or water or $[H_3O]^+$. Experiments carried out at −1.5 V versus Ag/AgCl revealed that deposition of Co(II) was possible, whereas assigning a potential of −1 V at the GC electrode did not yield any reduction of Co(II). It is worth highlighting that the electric charge is 0.3 and 14 C for the undiluted and diluted ABS−AcABSs, respectively. As a result, even if the Faradaic yield is twice as high with the ABS−AcABS-diluted, more electrons will be devoted to the reduction of water in the latter system. However, the cobalt deposition kinetics is more than 24 times faster in the diluted systems which significantly improves results obtained compared to pure ILs. After 1 h of chronoamperometric measurements, only 2.5 mol % Co(II) ions were reduced. This proves that the bath did not suffer from any significant concentration depletion. Larger surface electrodes are required to recover the metal in an acceptable length of time. The current−time transient for the deposition of Co(II) from the ABS−AcABS-diluted system was studied to determine the nucleation process (Figure S7 of the SI) and was found to follow a 3D instantaneous nucleation growth process.

The crystalline structures of the deposits obtained at the end of the chronoamperometry experiments were analyzed by XRD analysis with the spectra depicted in Figure 8. NaCl crystals are highlighted in the ABS−AcABS and ABSs. This is not surprising as these two solutions contain an important initial NaCl concentration (7.6 wt %) to induce the formation of two phases. Near the electrode, the deposition of cobalt in ABS−AcABS and ABSs will most likely release chloride anions from the metallic complexes and locally saturate the solution in NaCl inducing the crystallization of the latter salt. All deposits are composed of metallic Co(0) crystallized in a hexagonal close packed lattice. However, there are differences in the crystallization of Co(0) in the ABS and ABS−AcABS compared to the ABS−AcABS-diluted system. Focusing on the cobalt metallic peaks 2 (p_2) and 3 (p_3) at 44.6° and 47.5°, respectively, the ratio $R = p_2/p_3$ differs from one system to another. These two peaks correspond to the crystal orientation (111) and (101), respectively, of metallic cobalt.[34] Concerning the ABS−AcABS-diluted system, p_2 presents a higher intensity than p_3 resulting in a ratio R of 1.51. The opposite phenomenon is reported for ABS−AcABS and ABSs leading to a ratio of 0.51 and 0.47, respectively. This phenomenon highlights a preferential crystalline orientation of metals electrodeposited in concentrated IL solutions compared to diluted IL solutions. Such changes in the crystalline nature of deposits due to the presence of IL were previously reported for the deposition of copper in the presence of $[C_4mim][HSO_4]$ as additive.[35]

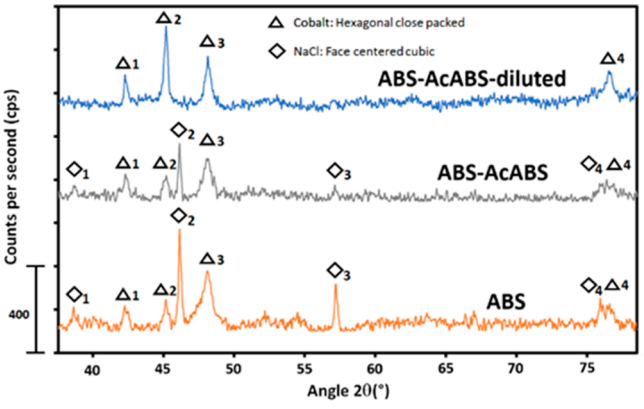

Figure 8. XRD diffractograms of deposits obtained after extraction of metals from a mixed solution containing 0.1 mol L^{-1} Co(II), Ni(II), and Mn(II) and electrodeposition at a potential of −2.00 V vs Ag/AgCl during 1 h.

The versatility of IL-based ABS and AcABS was recently highlighted for its application in metal extraction,[6,8,36,37] but it is here shown that it can be extended to the electrodeposition of metals. The hydrophilicity of the extracting solution allows the tuning and enhancement of the efficiency of the recovery of pure cobalt and modification of the properties of the resulting deposits.

CONCLUSIONS

AcABS and its ABS−AcABS derivative stand out as an efficient, flexible, and integrated extraction−separation−purification platform for the recovery of critical metals from primary and secondary ores. Upon varying of the HCl concentration and the chloride source (either NaCl or HCl), selective separation of Co(II) from Ni(II) was achieved while controlling the partition of the various system constituents. The distribution of HCl was found to have a profound influence on the subsequent electrodeposition of Co(II). To address this, a mixed ABS−AcABS extraction system was proposed which combines the advantages of the AcABS and ABSs. By varying the water content of the $[P_{44414}]$Cl-rich phase after extraction and separation of Co(II) from Ni(II), high-quality dendritic deposits of pure metallic cobalt were obtained in the presence of Mn(II) impurities. Furthermore, ABS−AcABSs can be tailored to obtain metal deposits with varied properties. The results presented in this work demonstrate the applicability of AcABS for a "one-pot" approach for the sequential leaching,

DOI: 10.1021/acssuschemeng.8b05754
ACS Sustainable Chem. Eng. 2019, 7, 1769−1777

solvent extraction, and electrodeposition of metals. Moreover, this work provides an understanding of the fundamental mechanisms governing the extraction and electrodeposition in AcABS required to extend these findings to the recovery of other critical metals.

■ ASSOCIATED CONTENT

Supporting Information

The Supporting Information is available free of charge on the ACS Publications website at DOI: 10.1021/acssuschemeng.8b05754.

Detailed list of chemicals and instruments used; extraction of Co(II), Ni(II), and Mn(II) in AcABS as a function of HCl concentration; IL-rich phase viscosity before and after Co(II) extraction; extraction in AcABS as a function of Co(II) concentration; composition of IL-rich phase after extraction in ABS and ABS−AcABSs; and nucleation mechanism (PDF)

■ AUTHOR INFORMATION

Corresponding Authors

*E-mail: nicolas.papaiconomou@lepmi.grenoble-inp.fr. Phone: +33 (0)6 81 91 17 57.

*E-mail: jcoutinho@ua.pt. Phone: ++351 234 401 507.

ORCID

Nicolas Schaeffer: 0000-0002-0747-2532

Helena Passos: 0000-0002-0573-093X

João A.P. Coutinho: 0000-0002-3841-743X

Author Contributions

§N.S. and M.G. are equally contributing authors. The manuscript was written through contributions of all authors. All authors have given approval to the final version of the manuscript.

Notes

The authors declare no competing financial interest.

■ ACKNOWLEDGMENTS

This work was part of BATRE-ARES Project (ERA-MIN/0001/2015) funded by ADEME and FCT. M.G. would like to acknowledge labex CEMAM and EIT InnoEnergy H2020 for financial support. This work was partly developed within the scope of the Project CICECO-Aveiro Institute of Materials, POCI-01-0145-FEDER-007679 (FCT ref. UID/CTM/50011/2013), financed by national funds through the FCT/MEC and when appropriate cofinanced by FEDER under the PT2020 Partnership Agreement.

■ REFERENCES

(1) Ayres, R. U. Metals *Recycling*: Economic and Environmental Implications. *Resour. Conserv. Recy.* **1997**, *21*, 145−173.

(2) Cui, J.; Forssberg, E. Mechanical recycling of waste electric and electronic equipment: a review. *J. Hazard. Mater.* **2003**, *99*, 243−263.

(3) Nuss, P.; Eckelman, M. Life Cycle Assessment of Metals: A Scientific Synthesis. *PLoS One* **2014**, *9*, No. e101298.

(4) Cui, J.; Zhang, L. Metallurgical recovery of metals from electronic waste: a review. *J. Hazard. Mater.* **2008**, *158*, 228−256.

(5) Wilson, A. M.; Bailey, P. J.; Tasker, P. A.; Turkington, J. R.; Grant, R. A.; Love, J. B. Solvent extraction: the coordination chemistry behind extractive metallurgy. *Chem. Soc. Rev.* **2014**, *43*, 123−134.

(6) Gras, M.; Papaiconomou, N.; Schaeffer, N.; Chainet, E.; Tedjar, F.; Coutinho, J. A. P.; Billard, I. Ionic-Liquid-Based Acidic Aqueous Biphasic Systems for Simultaneous Leaching and Extraction of Metallic Ions. *Angew. Chem., Int. Ed.* **2018**, *57*, 1563−1566.

(7) Hallett, J. P.; Welton, T. Room-temperature ionic liquids: solvents for synthesis and catalysis. 2. *Chem. Rev.* **2011**, *111*, 3508−3576.

(8) Onghena, B.; Opsomer, T.; Binnemans, K. Separation of cobalt and nickel using a thermomorphic ionic-liquid-based aqueous biphasic system. *Chem. Commun.* **2015**, *51*, 15932−15935.

(9) Shahriari, S.; Neves, C. M. S. S.; Freire, M. G.; Coutinho, J. A. P. Role of the Hofmeister Series in the Formation of Ionic-Liquid-Based Aqueous Biphasic Systems. *J. Phys. Chem. B* **2012**, *116*, 7252.

(10) Thuy Pham, T. P.; Cho, C. W.; Yun, Y. S. Environmental fate and toxicity of ionic liquids: a review. *Water Res.* **2010**, *44*, 352.

(11) Fu, J.; Yang, Y. I.; Zhang, J.; Chen, Q.; Shen, X.; Gao, Y. Q. Structural Characteristics of Homogeneous Hydrophobic Ionic Liquid−HNO_3−H_2O Ternary System: Experimental Studies and Molecular Dynamics Simulations. *J. Phys. Chem. B* **2016**, *120*, 5194.

(12) Mazan, V.; Boltoeva, M. Y.; Tereshatov, E. E.; Folden, C. M., III Mutual solubility of water and hydrophobic ionic liquids in the presence of hydrochloric acid. *RSC Adv.* **2016**, *6*, 56260.

(13) Vander Hoogerstraete, T.; Wellens, S.; Verachtert, K.; Binnemans, K. Removal of transition metals from rare earths by solvent extraction with an undiluted phosphonium ionic liquid: separations relevant to rare-earth magnet recycling. *Green Chem.* **2013**, *15*, 919.

(14) Wellens, S.; Thijs, B.; Binnemans, K. An environmentally friendlier approach to hydrometallurgy: highly selective separation of cobalt from nickel by solvent extraction with undiluted phosphonium ionic liquids. *Green Chem.* **2012**, *14*, 1657−1665.

(15) European Commission. *Study on the review of the list of Critical Raw Materials*; Publications Office of the European Union: Luxembourg, 2017. DOI: 10.2873/876644.

(16) Larsson, K.; Binnemans, K. Selective extraction of metals using ionic liquids for nickel metal hydride battery recycling. *Green Chem.* **2014**, *16*, 4595−4603.

(17) Neves, C. M. S. S.; Ventura, S. P. M.; Freire, M. G.; Marrucho, I. M.; Coutinho, J. A. P. Evaluation of Cation Influence on the Formation and Extraction Capability of Ionic-Liquid-Based Aqueous Biphasic Systems. *J. Phys. Chem. B* **2009**, *113*, 5194−5199.

(18) Högfeldt, E. *IUPAC Stability constants of metal-ion Complexes Part A: Inorganic ligands*; IUPAC; Pergamon Press, 1982.

(19) Schaeffer, N.; Passos, H.; Gras, M.; Mogilireddy, V.; Leal, J. P.; Pérez-Sánchez, G.; Gomes, J. R. B.; Billard, I.; Papaiconomou, N.; Coutinho, J. A. P. Mechanism of ionic-liquid-based acidic aqueous biphasic system formation. *Phys. Chem. Chem. Phys.* **2018**, *20*, 9838−9846.

(20) Onghena, B.; Valgaeren, S.; Vander Hoogerstraete, T.; Binnemans, K. Cobalt(II)/nickel(II) separation from sulfate media by solvent extraction with an undiluted quaternary phosphonium ionic liquid. *RSC Adv.* **2017**, *7*, 35992−35999.

(21) Papaiconomou, N.; Svecova, L.; Bonnaud, C.; Cathelin, L.; Billard, I.; Chainet, E. Possibilities and limitations in separating Pt(IV) from Pd(II) combining imidazolium and phosphonium ionic liquids. *Dalton Trans.* **2015**, *44*, 20131−20138.

(22) Hsieh, Y. T.; Lai, M. C.; Huang, H. L.; Sun, I. W. Speciation of cobalt-chloride-based ionic liquids and electrodeposition of Co wires. *Electrochim. Acta* **2014**, *117*, 217−223.

(23) Tsunashima, K.; Sugiya, M. Physical and electrochemical properties of low-viscosity phosphonium ionic liquids as potential electrolytes. *Electrochem. Commun.* **2007**, *9*, 2353−2358.

(24) MacFarlane, D. R.; Tachikawa, N.; Forsyth, M.; Pringle, J. M.; Angell, C. A. Energy applications of ionic liquids. *Energy Environ. Sci.* **2014**, *7*, 232−250.

(25) Bard, A.; Parsons, J.; Jordan, R. *Standard potentials in aqueous solutions*; CRC Press, 1985.

(26) Lechat, S.; Khan, M. A.; Bouet, G. Spectrophotometric study of cobalt(II) chloride complexes in ethanol and propan-2-ol. *Inorg. Chim. Acta* **1993**, *211*, 33−36.

(27) Matulis, J.; Slizys, K. On Some Characteristics of Cathodic Processes in Nickel Electrodeposition. *Electrochim. Acta* **1964**, *9*, 1177−1188.
(28) Piatti, R. C. V.; Arvia, A. J.; Podesta, J. J. The Electrochemical Kinetic Behaviour of Nickel in Acid Aqueous Solutions Containing Chloride and Perchlorate Anions. *Electrochim. Acta* **1969**, *14*, 541−560.
(29) Chassaing, E.; Joussellin, M.; Wiart, R. The Kinetics of Nickel Electrodeposition Inhibition by Adsorbed Hydrogen and Anions. *J. Electroanal. Chem. Interfacial Electrochem.* **1983**, *157*, 75−88.
(30) Suryanto, B. H. R.; Lu, X.; Chan, H. M.; Zhao, C. Controlled electrodeposition of cobalt oxides from protic ionic liquids for electrocatalytic water oxidation. *RSC Adv.* **2013**, *3*, 20936−20942.
(31) Crundwell, F. K.; Moats, M.S.; Ramachandran, V.; Robinson, T.G.; Davenport, W.G. *Extractive metallurgy of nickel, cobalt and platinum group metals*; Elsevier, 2011.
(32) Abbott, A. P. Model for the Conductivity of Ionic Liquids Based on an Infinite Dilution of Holes. *ChemPhysChem* **2005**, *6*, 2502−2505.
(33) Kornyshev, A. A. Double-Layer in Ionic Liquids: Paradigm Change? *J. Phys. Chem. B* **2007**, *111*, 5545−5557.
(34) Qin, W.; Yang, C.; Ma, X.; Lai, S. Selective synthesis and characterization of metallic cobalt, cobalt/platinum, and platinum microspheres. *J. Alloys Compd.* **2011**, *509*, 338−342.
(35) Zhang, Q. B.; Hua, Y. X.; Wang, Y. T.; Lu, H. J.; Zhang, X. Y. Effects of ionic liquid additive $[BMIM]HSO_4$ on copper electrodeposition from acidic sulfate electrolyte. *Hydrometallurgy* **2009**, *98*, 291−297.
(36) Blesic, M.; Nimal Gunaratne, H. Q.; Jacquemin, J.; Nockemann, P.; Olejarz, S.; Seddon, K. R.; Strauss, C. R. Tunable thermomorphism and applications of ionic liquid analogues of Girard's reagents. *Green Chem.* **2014**, *16*, 4115−4121.
(37) Vander Hoogerstraete, T.; Onghena, B.; Binnemans, K. Homogeneous Liquid−Liquid Extraction of Metal Ions with a Functionalized Ionic Liquid. *J. Phys. Chem. Lett.* **2013**, *4*, 1659−1663.

DOI: 10.1021/acssuschemeng.8b05754
ACS Sustainable Chem. Eng. 2019, 7, 1769−1777